Microsystem Technologies (2021) 27:3875–3891
https://doi.org/10.1007/s00542-020-05184-y

TECHNICAL PAPER

# The use of roll-to-plate UV-curing embossing to produce a composite light guide plate

Cheng-Hsien Wu[1] · Yu-Cheng Liou[1]

Received: 7 December 2020 / Accepted: 11 December 2020 / Published online: 5 January 2021


**Abstract**
Roll-to-roll technology is used to form optoelectronic products because it allows fast, continuous production and a short cycle time. It has become the mass production technology with the most potential for development for the production of plastic products with a microstructure. This study designs and manufactures a composite light guide plate (LGP) to replace a traditional LGP with two pieces of prism sheet. The bottom surface of the composite LGP features dot microstructures and the upper surface features prism microstructures. The optical design is optimized separately for the dot microstructure and the prism microstructure. T he optimum designs are used to produce a composite LGP. One side uses the optimized dot distribution, and the other side uses pyramid microstructures. A PMMA substrate with a thickness of 2 mm is manufactured using roll-to-plate UV-cured embossing. In order to manufacture LGPs with microstructures on both sides, a rolling machine with an adjustment and positioning function is manufactured. Taguchi analysis is used to determine the single-sided optimized parameters. The dot structure is replicated 97% and the pyramid structure is replicated 96%. The proposed design for a composite light guide plate with a double-sided structure significantly increases the central average brightness and the uniformity of luminance.

## 1 Introduction

Thin film transistor-liquid crystal displays (TFT-LCDs) feature high brightness, thin dimension, and low power consumption (Feng et al. 2004). A backlight system converts a linear light source into an area of uniform light. A conventional LCD backlight system is composed of light sources, a light guide plate (LGP) and optical films, such as reflective sheets, diffusion sheets or prism sheets. This system has a surface onto which light is incident at one side of the LGP. The light is totally internal reflected and refracted by an array of etched or ink-printed white spots at the bottom of the LGP (reflecting surface). The light that emanates from the top surface of the LGP (emergence surface) is dispersed by the diffusion sheet, which reduces the intensity of bright or dark fringes that are made by spots (Wu and Liou 2008).

✉ Cheng-Hsien Wu
chengwu@nkust.edu.tw

[1] Department of Mold and Die Engineering, National Kaohsiung University of Science and Technology, Kaohsiung 807, Taiwan

The prism reshapes the backlight's luminance distribution. It collimates the light by refracting rays on the surface of the one-dimensional micro prism, which increases the on-axis luminance (Yang and Huang 2013). Recently, many studies have made LCD's thinner, brighter and more lightweight, with better backlight systems.

All parts in a backlight system, including the LGP, must have superior optical performance so a very accurate shape must be replicated and there must be low optical anisotropy from the stress due to molding.

The microstructure of a light guide plate can include a single-layer, multiple layers and composite structures. A single-layer microstructure is directly embossed onto the surface of the substrate. Most current units are single-layer microstructures, as shown in Fig. 1a. Multi-layer microstructures have a single-layer structure molding, onto which other layers are stacked to form the second-layer structure, as shown in Fig. 1b. A composite structure is a multi-faceted microstructure molding on a single substrate, as shown in Fig. 1c. The optical simulation and manufacturing processes for a composite structure are discussed.

A LGP is produced by injection molding or hot embossing. An important advantage of injection molding is that it can be used to make complex geometries in a single

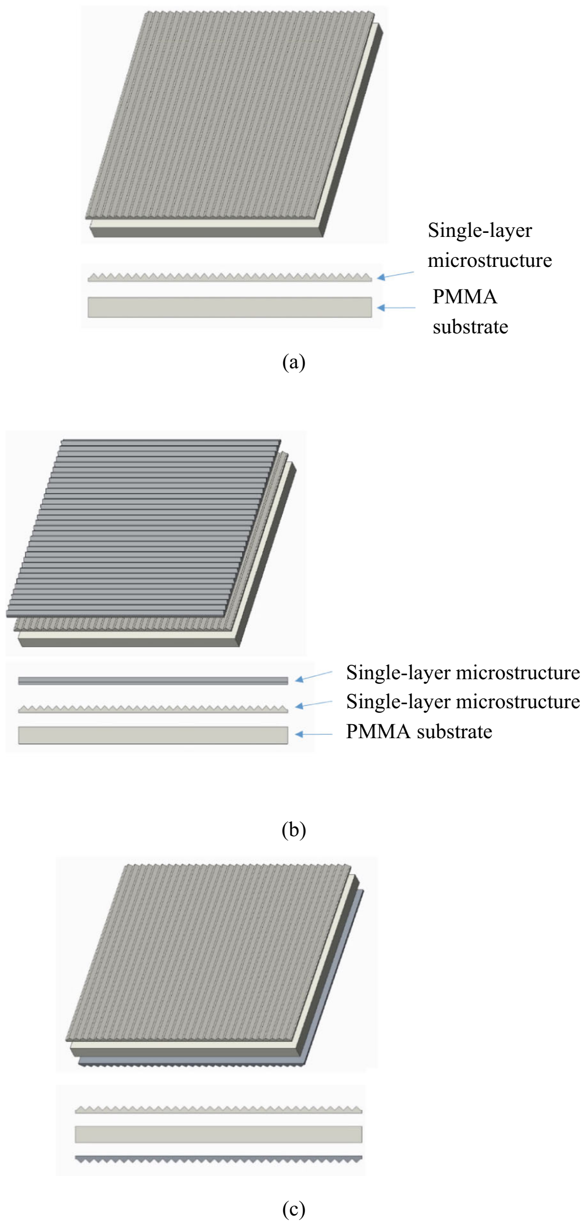


**Fig. 1** LGP with **a** single-layer, **b** multi-layer and **c** composite structure

production step using an automated process. However, the injection molding process has some inherent problems in terms of the molding of micro-features (Yao and Kim 2002). Hot embossing is used to fabricate plastic microstructures with high precision and high quality and is currently used for a few optical applications. The advantages of hot embossing are low material flow, low internal stress, which reduces defects in optical applications, and low flow rates (Heckele et al. 1998), so more delicate structures can be fabricated. The process is not suited to high production rates so it is not widely applicable.

Embossing processes use a flat embossing master so have a limited capability in large-area production. A large-area stamp has a specific criterion for surface flatness and applying a uniform pressure across the entire embossing surface is difficult, so it is not easy to achieve a consistent feature size. Large-area microstructures are also difficult to release from a flat mold (Chan-Park and Neo 2003).

In terms of micro-forming technologies, UV-curing is used for polymer processing at low temperature. Ultraviolet (UV) embossing is a replication technique that requires only a low temperature and low pressure for molding. UV embossing involves molding against micro-structured molds and is a quick and efficient method to mass produce high aspect ratio micro-features (Chan-Park and Neo 2003). Using a UV-curable resin as an embossing material, micro/nano features with high aspect ratios of more than 10 and a resolution of 50 nm can be embossed (Nezuka et al. 2008; Yeo et al. 2009; Gates et al. 2005).

Roll embossing with UV-curing is used to manufacture polymer products with microstructures to increase productivity. A flat mold is replaced by a roller to continuously emboss large-area patterns. UV-curable resin is evenly applied onto a plastic substrate and then a series of rollers are used to carry the substrate to the bottom of the roller. The microstructure on the roller is embossed on the UV resin above the transparent substrate using the tension of the film. A UV light below the roller irradiates and cures the embossed resin. The substrate can be either a roll of film or a plate. This process is called UV-cured roll-to-roll embossing if the substrate is a roll of film. It is called UV-cured roll-to-plate embossing if the substrate is a flat plate. Common UV-curing molding technologies include plate-to-plate, roll-to-roll, roll-to-plate and micro embossing.

Experiments are performed to determine the effect of the formation of a meniscus on a roll-to-roll ultraviolet (UV) embossing process. Adjusting the slot-die coater pressure can prevent formation of a meniscus and a perfect negative copy of the mold is imprinted on the embossed substrate (Zhong and Shan 2014). This technology allows fast production, mass production, a short molding cycle, accurate replication and high precision. It is suited to forming optoelectronic components and biomedical products that feature a precise microstructure.

Combining the functions of a traditional light guide plate and the two prism sheets, a composite light guide plate is designed for this study. Instead of a traditional V-cut structure, the light guide plate has a dot array on one side and a pyramid microstructure on the other side. A 2 mm-thick PMMA substrate is manufactured using UV-cured roll-to-plate embossing, which prevents film positioning errors during assembly. The luminance of a traditional light guide plate assembled is compared with that for a prism film and a composite light guide plate with a double-sided structure.

## 2 Optical design

The optical analysis software, TracePro 7.3 (Lambda Research Corporation, USA), is used for the optical simulation of a backlight module. The simulation involves an optical analysis of a single-sided dot array and a single-sided prism microstructure. The dot array is shown in Fig. 2a and various prism microstructures, including a double-layer V-cut, pyramid type and inverted pyramid type, are shown in Fig. 2b–d. The composite microstructure is then simulated. The composite microstructure is a dot array on one side and a prism array on the other side.

The configuration of the backlight module for this study is shown in Fig. 3. There are six LEDs in total: three on each side. The illuminance and luminance are measured at 9 points, as shown in Fig. 4. The measurement data is used to calculate the relative value, based on the central point. Optical uniformity is determined by the relative luminance of these nine points. The relative luminance is calculated as:

$$\text{Relative luminance} = \frac{\text{luminance at any point}}{\text{luminance at central point}} \times 100\%.$$

### 2.1 Dot microstructure arrangement design

This study determines the best microstructure to give uniform divergence for six LEDs. An optical analysis determines the divergence of the unstructured LGP, as shown in Fig. 5. The luminance is greater near the LED light source so microstructures are added to change the optical properties of the LGP and allow the light to diffuse uniformly.

The DOT on the LGP refracts and scatters light. This study uses a hemispherical dot with a diameter of 1 mm and a depth of 0.47 mm, as shown in Fig. 6. Each dot is on a tangent to another, which is called DOT-1, as shown in Fig. 7a. The LED light source is located on both sides so the direction of light scattering is critical to achieving uniformity across the substrate. The optical analysis shows that the structure is concentrated in the middle so the middle is brighter than the sides. Therefore, the two rows of dots outside DOT-1 are moved 1.74 mm outward to form DOT-2. Similar modification is required for DOT-3, DOT-4 and DOT-5. This study uses five dot structure distributions, as shown in Fig. 7, and the scattering data is compared to determine the best distribution.

### 2.2 V-cut microstructure design

The prism sheet guides light. A traditional backlight module uses two mutually perpendicular V-cut prisms to

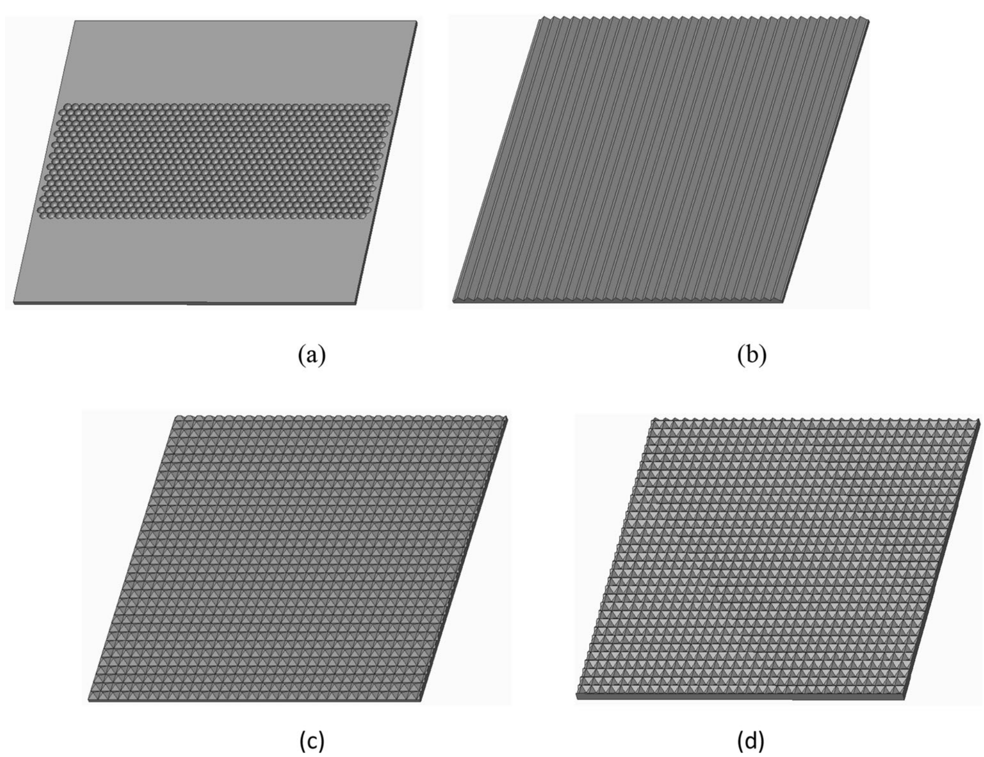

Fig. 2 LGP with **a** DOT, **b** double-layer of V-cut, **c** pyramid and **d** inverted pyramid structure

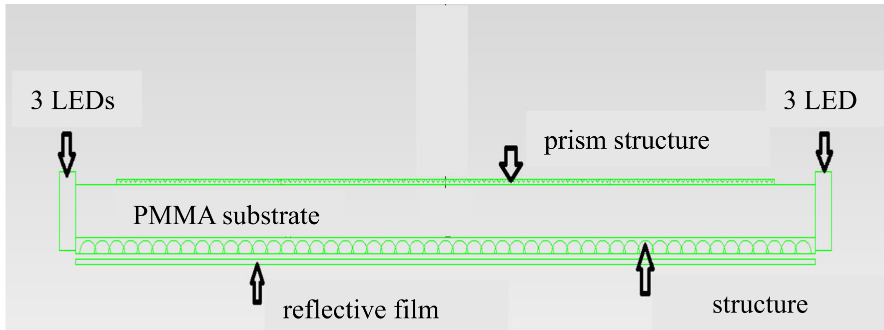


Fig. 3 Configuration of the backlight module

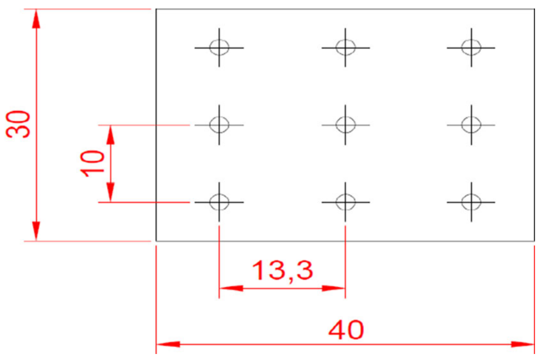


Fig. 4 Nine measurement locations

guide light. Preliminary testing showed that an angle for the V-cut of 104° gives the greatest increase in luminance. This study uses a composite structure, instead of two orthogonal prism sheets.

To minimize manufacturing costs for the microstructure, the V-cut structure has a side length of 0.6 mm, a height of 0.234 mm and an angle of 104°, as shown in Fig. 8. If two mutually perpendicular V-cut arrays are superimposed, a pyramid or inverted pyramid microstructure is produced. Optical analysis was performed to compare the light-gathering effects of these three types of prisms. The Double-layers of V-cut are shown in Fig. 9a, the pyramid microstructure is shown in Fig. 9b and the inverted pyramid microstructure is shown in Fig. 9c.

The composite LGP includes an upper layer with a prism structure, a middle substrate and a lower layer with a dot structure. The composite structure guides the refraction and reflection of light to achieve uniform light distribution. The luminance at 9 points was measured to determine the effect of the microstructure on the average luminance and its uniformity.

The panel size for this study is 40 mm × 30 mm. At the bottom of the light guide plate, different dot distributions are used to determine the effect of the distribution on light gathering. The simulation results for the luminance distribution for the unstructured light guide plate are shown in Fig. 5. The average luminance value is 198 nit. The nine-

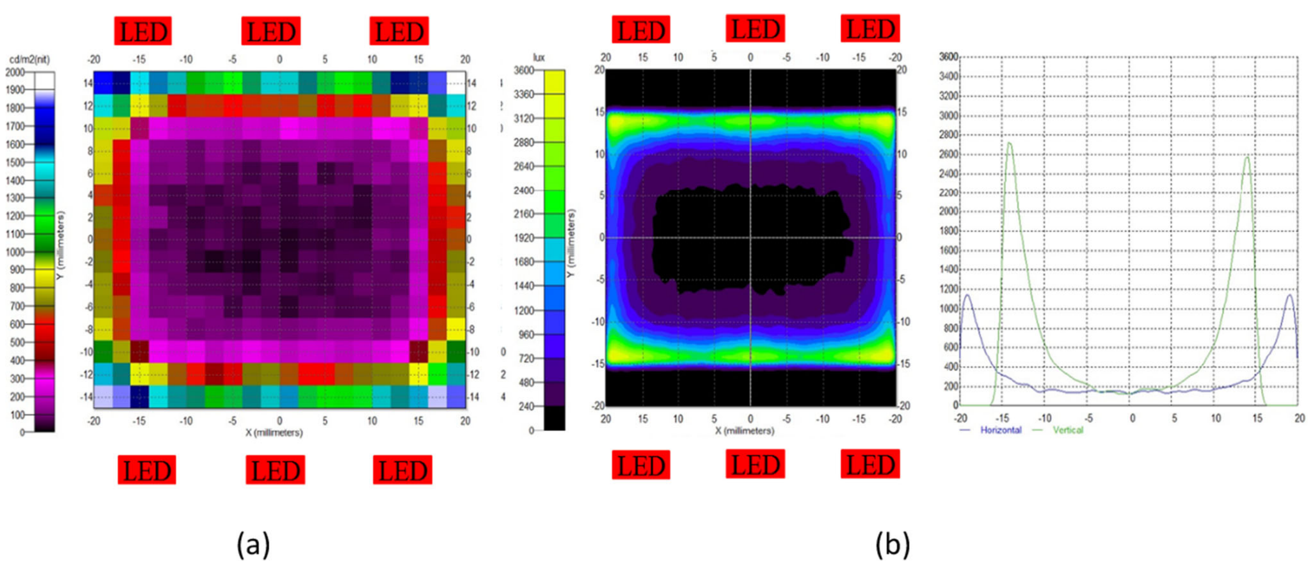


Fig. 5 **a** Luminance and **b** illuminance of an unstructured LGP point measurement values for luminance are shown in Table 1.

For the unstructured light guide plates with microstructure distributions of DOT-1, DOT-2, DOT-3, DOT-4 and DOT-5 feature an average respective increase in luminance of about 3.9 times, 9.7 times, 8.7 times, 8.1 times and 6.7 times. The uniformity is calculated as the difference between the maximum value and the minimum value. The luminance maps for DOT-1 and DOT-2 show that the luminance on the side that is adjacent to the light source is too low, so the overall luminance is uneven, as shown in Fig. 10 and Tables 2, 3. Therefore, the design for DOT-1 and DOT-2 is not used. The results show that DOT-3 and DOT-4 feature better luminance and DOT-5 has the next best result.

The effect of different microstructures for the LGP on light-guiding is determined. LGPs with double-layers of V-cut, pyramid and inverted pyramid microstructure have an average luminance that is about 5.0 times, 6.0 times and 5.2 times greater than that for an unstructured LGP.

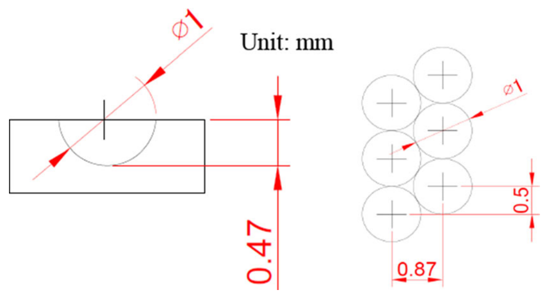


**Fig. 6** Dimensions of DOT structures

## 2.3 Analysis of the composite structure

A light guide plate with a composite structure was manufactured. The bottom surface uses a DOT microstructure to refract and reflect light to achieve uniform light distribution. The middle is a PMMA substrate. The microstructure for the upper surface features a prism structure to guide the light. The luminance at the specified 9 points was measured to determine the effect of the combination of microstructures on the luminance and uniformity.

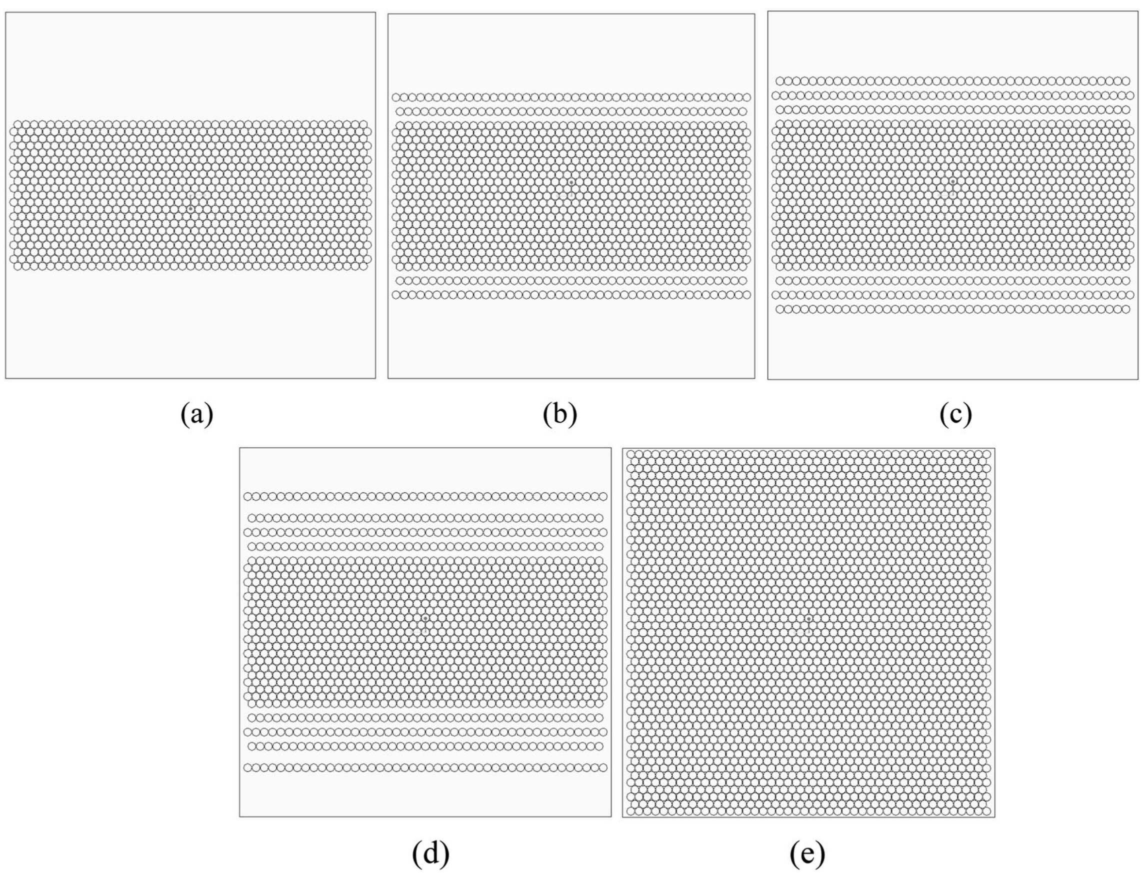


**Fig. 7** Five designs for various dot distributions

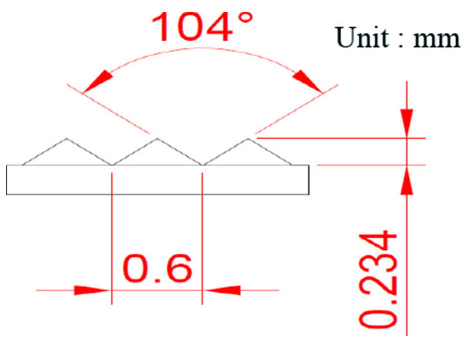


**Fig. 8** Dimensions of V-cut structures

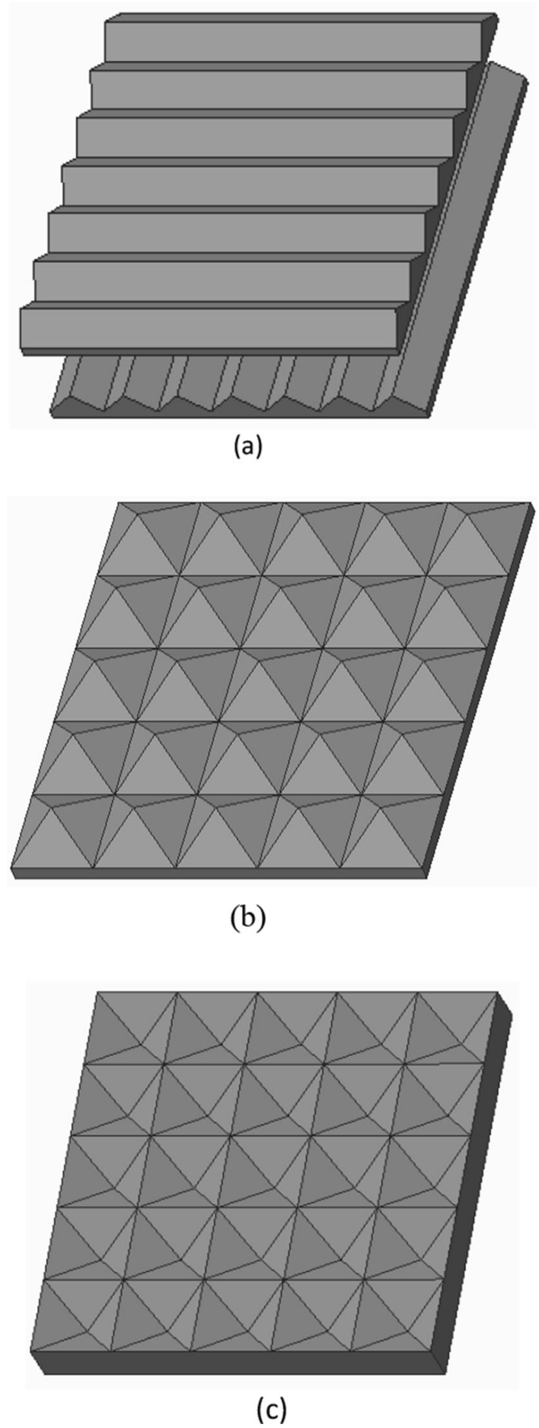


**Fig. 9** **a** Double-layers of V-cut, **b** pyramid and **c** inverted pyramid microstructures

The first structure has an upper surface for the LGP that features a double-layer V-cut structure and the lower surface features various dot arrays. Light guide plates with DOT-3, DOT-4 and DOT-5 microstructure distributions have an average luminance that is about 8.8 times, 8.1 times and 7.1 times higher than that for an unstructured light guide plate.

The second structure has an upper surface for the light guide plate that features a pyramid microstructure and the lower surface features various dot arrays. Light guide plates with DOT-3, DOT-4 and DOT-5 microstructure distributions have an average luminance that is about 9.4 times, 8.0 times and 7.1 times higher than an unstructured light guide plate.

The final structure has an upper surface for the light guide plate that features an inverted pyramid microstructure and the lower surface features various dot arrays. Light guide plates with DOT-3, DOT-4 and DOT-5 microstructure distributions have an average luminance that is about 8.8 times, 7.8 times and 6.2 times higher than unstructured light guide plates.

A comparison of the average luminance for the composite LGP with various combinations of microstructure is shown in Table 4. DOT-3 and the pyramid microstructure are the best fit. This study uses this microstructure design for the light guide plate. When the light guide plate was manufactured, the optical properties were measured.

## 3 Experimental

A roll-to-plate UV-curing embossing machine that was developed in the authors' laboratory was used to form the microstructure. The optimization results show that a DOT-3 microstructure on the upper surface and a pyramid microstructure on the lower surface give the best results. A series of roll-to-plate UV-curing embossing cycles were used to optimize the process parameters.

**Table 1** Luminance data for an unstructured LGP (unit: nit)

| Nine points of luminance | | | | Relative luminance (%) | | |
|---|---|---|---|---|---|---|
| 262 | 250 | 275 | | 672 | 641 | 705 |
| 68 | 39 | 90 | Average | 174 | 100 | 231 |
| 277 | 217 | 305 | 198 | 710 | 556 | 782 |

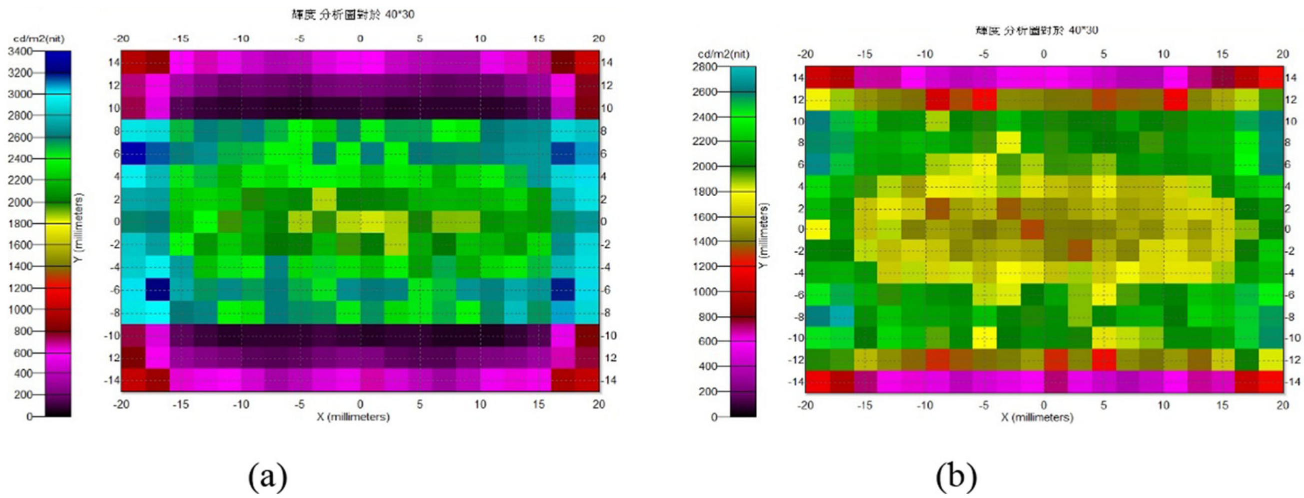


**Fig. 10** Luminance of LGP with (**a**) DOT-1 and (**b**) DOT-2 microstructure

**Table 2** Luminance data for a LGP with DOT-1 microstructure (unit: nit)

| Nine points of luminance | | | | Relative luminance (%) | | |
|---|---|---|---|---|---|---|
| 98 | 94 | 93 | | 5 | 5 | 5 |
| 2397 | 1847 | 2124 | Average | 130 | 100 | 115 |
| 106 | 78 | 90 | 770 | 6 | 4 | 5 |

**Table 3** Luminance data for a LGP with DOT-2 microstructure (unit: nit)

| Nine points of luminance | | | | Relative luminance (%) | | |
|---|---|---|---|---|---|---|
| 2070 | 2024 | 2121 | | 152 | 148 | 155 |
| 1861 | 1366 | 1504 | Average | 136 | 100 | 110 |
| 2277 | 2063 | 2056 | 1927 | 167 | 151 | 151 |

**Table 4** Average luminance comparison of composite LGPs with various combinations (unit: nit)

| Upper surface / Lower surface | Double-layer V-cut | Pyramid | Inverted pyramid |
|---|---|---|---|
| DOT-3 | 1742 | 1867 | 1733 |
| DOT-4 | 1601 | 1584 | 1554 |
| DOT-5 | 1410 | 1407 | 1230 |

## 3.1 Materials

An optical grade PMMA sheet with a size of 70 mm × 70 mm × 2 mm was used as the substrate. The microstructure was manufactured by coating UV resin (PMMA 80471, Eternal Materials Co., Taiwan) onto a piece of PMMA substrate and then embossing with a roller. The refractive index of the substrate is 1.49 and 1.47 for the UV resin at a temperature of 25 °C.

## 3.2 Manufacturing processes

Roll-to-plate processes were used to produce a LGP for this study. After coating the plate with UV resin, the coated plate was transferred through a roller with a specific microstructure. After curing using UV light irradiation, a micro-structured plate is formed, as shown in Fig. 11.

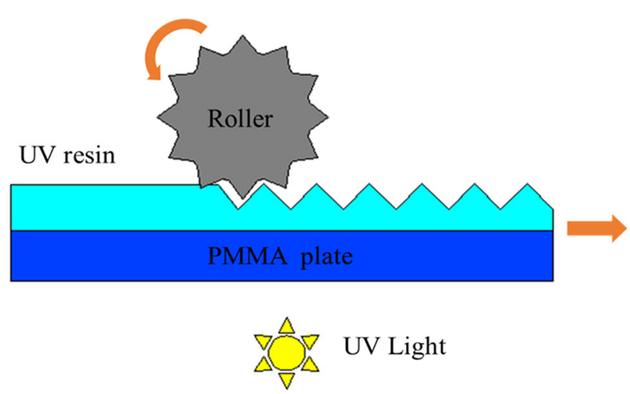


**Fig. 11** Roll-to-plate UV-curing embossing processes

### 3.3 Roll-to-plate UV-curing embossing machine

The roll-to-plate UV-curing embossing machine used automation, intelligence and modularization. The machine was controlled using the LabVIEW program. The roller position and the rolling process parameters were fine-tuned to ensure a stable roll-to-plate UV-curing embossing process.

There are different sheet thicknesses so the roller must be adjustable in height. The embossing machine also controls horizontal positioning for double-sided embossing. The composite light guide plate requires double-sided roll-embossing so the UV-curing embossing machine must ensure that the horizontal position of the roller is correct. After roll-embossing the first side, the relative position of the roller and the plastic plate must be adjusted before rolling the second side to align positions of the microstructures on both sides. The design and a photograph of the machine are shown in Fig. 12.

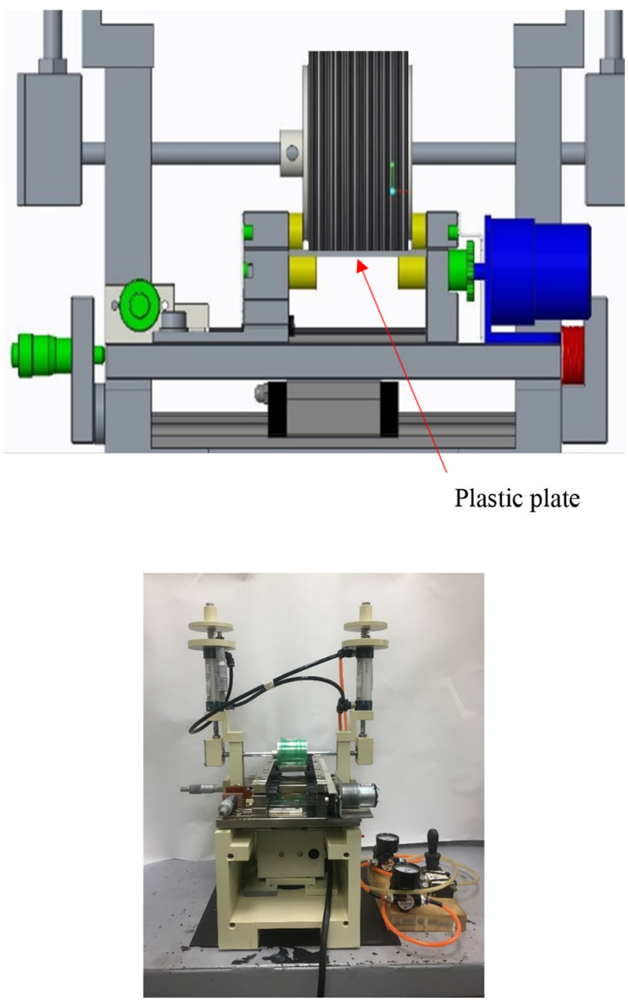


Fig. 12 Design and photo of a roll-to-plate UV-curing embossing machine

During the embossing process, the start and end times for ultraviolet light irradiation have a significant effect on the formability of the structure. If the UV resin is irradiated too early, it hardens prematurely so it cannot be embossed. If the irradiation of the UV resin begins too late or ends too early, the material is not cured properly and fails to harden completely. Therefore, the switch control for UV light irradiation is very important. This study uses a bespoke design for the UV light shielding plate.

When the mold wheel rolls over the substrate, UV light irradiates the UV resin on the substrate to cure it. The speed of the conveying wheel determines the appropriate start and end time for UV light irradiation. This is controlled by adjusting the shielding plates. Adjustment of a shielding plate is precisely fine-tuned using a micrometer head, as shown in Fig. 13. The UV start and end times for light irradiation control the degree of curing.

The position of the front shielding plate controls the start time. The distance between the front shielding plate and the rear shielding plate depends on the speed at which the coated substrate moves and the duration of the irradiation.

### 3.4 Roller manufacture

The microstructure is printed on the surface of the LGP so the embossing experiments for this study use the roll-to-plate UV-curing embossing machine that was developed in the authors' laboratory. In the embossing processes, the

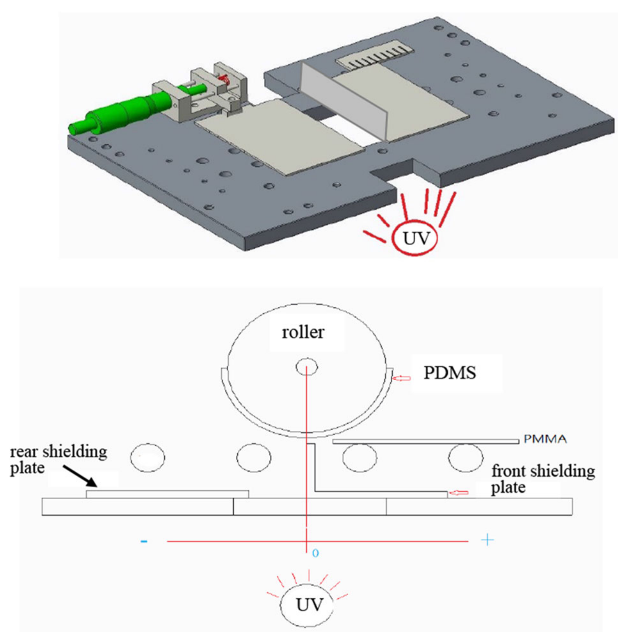


Fig. 13 Adjustment of the shading plate is fine-tuned using a micrometer head

micro-structured roller was manufactured first and then the microstructure on the roller was reprinted on the LGP using the roll-to-plate machine. TO reduce production costs and increase practicability, the PDMS soft template was affixed to an aluminum roller.

The following steps were used to manufacture a roller with microstructures.

1. A precision CNC machine was used to machine the microstructure on a steel plate, as shown in Fig. 14a.
2. The main agent for PDMS was mixed with the hardener and the mixture was held under vacuum to remove small bubbles that are generated by stirring. The mixture was then poured onto the machined steel plate. A piece of glass was covered to make a soft PDMS insert with a uniform thickness of 2 mm, as shown in Fig. 14b.
3. This was placed on a heating plate at a temperature of 125 °C and heated for about 30 min to one hour to ensure a complete cure, as shown in Fig. 14c.
4. The soft PDMS insert was then affixed to an aluminum roller and the microstructure was printed on the light guide plate, as shown in Fig. 14d.

## 3.5 Process steps

For this study, roll-to-plate UV-curing embossing technology was used to form microstructures on a flat plate. The following are the process steps for this study.

1. The conveyor belt was raised to the proper position for the thickness of the sheet.
2. The shielding plate was moved to adjust the exposure time.
3. The two air pressure columns were adjusted by fine-tuning the micrometer head above the air column to ensure an even embossing pressure for the roller on the substrate.
4. The UV light source was switched on for 1.5 min to allow the UV light output energy to reach a steady state.
5. UV resin was poured onto the PMMA substrate, using the coating mechanism to control the thickness of the wet film.
6. The rolling and curing processes are shown in Fig. 15.

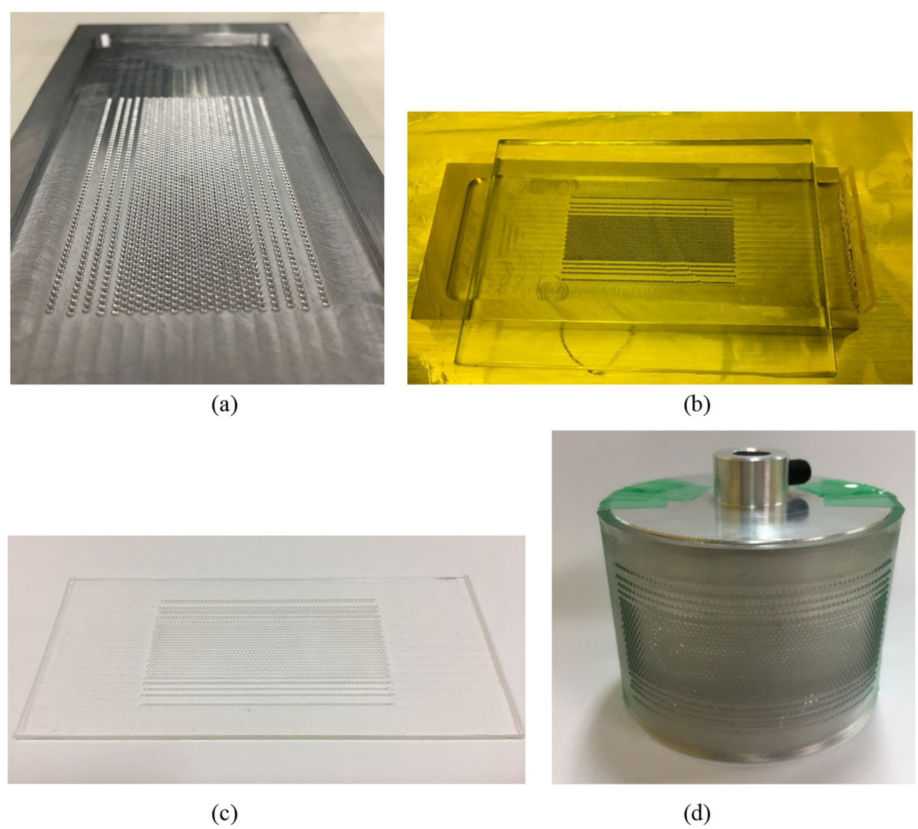


**Fig. 14** Steps for making a roller with microstructures

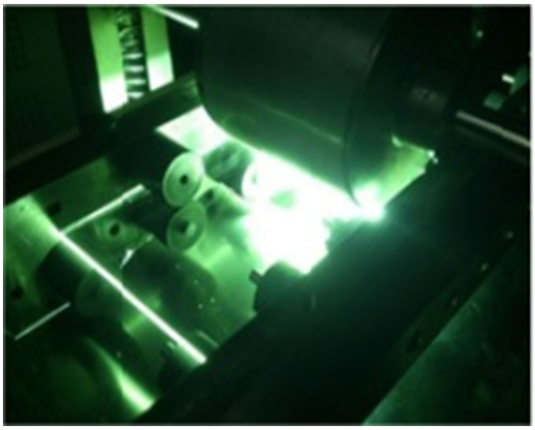

**Fig. 15** Roll-to-plate UV-curing embossing processes

**Table 5** Factors and levels for DOT-3 microstructures

| Factor | Level 1 | Level 2 | Level 3 |
|---|---|---|---|
| A (substrate speed, mm/s) | 3.6 | 4 | 4.5 |
| B (exposure time, s) | 0.75 | 1 | 1.5 |
| C (exposure position, mm) | − 1 | 0 | 1 |
| D (air pressure, kPa) | 637 | 686 | 735 |

**Table 6** Factors and levels for pyramid microstructures

| Factor | Level 1 | Level 2 | Level 3 |
|---|---|---|---|
| A (substrate speed, mm/s) | 3.6 | 4 | 4.5 |
| B (exposure time, s) | 0.75 | 1 | 1.5 |
| C (exposure position, mm) | 0 | 1 | 2 |
| D (air pressure, kPa) | 637 | 686 | 735 |

**Table 7** Measured replicability (y), standard deviation (s) and *S/N* ratio for DOT-3 microstructures

| Exp | A | B | C | D | $y_1$ | $y_2$ | $y_3$ | $y_{avg}$ | s | *S/N* |
|---|---|---|---|---|---|---|---|---|---|---|
| 1 | 1 | 1 | 1 | 1 | 92.00 | 91.56 | 91.11 | 91.56 | 0.45 | 39.23 |
| 2 | 1 | 2 | 2 | 2 | 92.89 | 92.00 | 92.44 | 92.44 | 0.45 | 39.32 |
| 3 | 1 | 3 | 3 | 3 | 93.78 | 91.56 | 92.89 | 92.74 | 1.12 | 39.34 |
| 4 | 2 | 1 | 2 | 3 | 87.11 | 86.67 | 88.44 | 87.41 | 0.92 | 38.83 |
| 5 | 2 | 2 | 3 | 1 | 93.33 | 93.33 | 94.22 | 93.63 | 0.51 | 39.43 |
| 6 | 2 | 3 | 1 | 2 | 92.00 | 91.56 | 92.44 | 92.00 | 0.44 | 39.28 |
| 7 | 3 | 1 | 3 | 2 | 93.33 | 93.78 | 93.78 | 93.63 | 0.26 | 39.43 |
| 8 | 3 | 2 | 1 | 3 | 92.89 | 94.22 | 94.22 | 93.78 | 0.77 | 39.44 |
| 9 | 3 | 3 | 2 | 1 | 92.44 | 93.78 | 94.22 | 93.48 | 0.93 | 39.41 |
| Average | | | | | | | | 92.30 | 5.84 | 39.30 |

**Table 8** Measured replicability (y), standard deviation (s) and *S/N* ratio for pyramid microstructures

| Exp | A | B | C | D | $y_1$ | $y_2$ | $y_3$ | $y_{avg}$ | s | *S/N* |
|---|---|---|---|---|---|---|---|---|---|---|
| 1 | 1 | 1 | 1 | 1 | 90.80 | 91.20 | 90.96 | 90.99 | 0.20 | 39.18 |
| 2 | 1 | 2 | 2 | 2 | 92.00 | 92.40 | 92.40 | 92.27 | 0.23 | 39.30 |
| 3 | 1 | 3 | 3 | 3 | 83.76 | 84.00 | 83.36 | 83.71 | 0.32 | 38.46 |
| 4 | 2 | 1 | 2 | 3 | 91.84 | 92.00 | 91.76 | 91.87 | 0.12 | 39.26 |
| 5 | 2 | 2 | 3 | 1 | 81.60 | 82.40 | 81.76 | 81.92 | 0.42 | 38.27 |
| 6 | 2 | 3 | 1 | 2 | 93.60 | 94.40 | 94.00 | 94.00 | 0.40 | 39.46 |
| 7 | 3 | 1 | 3 | 2 | 88.40 | 88.80 | 88.00 | 88.40 | 0.40 | 38.93 |
| 8 | 3 | 2 | 1 | 3 | 84.40 | 85.20 | 84.48 | 84.69 | 0.44 | 38.56 |
| 9 | 3 | 3 | 2 | 1 | 84.40 | 85.04 | 84.56 | 84.67 | 0.33 | 38.55 |
| Average | | | | | | | | 88.06 | 2.87 | 38.89 |

## 3.6 Process optimization

The Taguchi method was used for the roll-to-plate UV-curing embossing experiments to optimize the replicability of the finished product. Preliminary experiments determined the parameters that are control factors and the appropriate levels were selected. This experiment determined the optimal value for each control factor to determine the effect of each parameter on the replicability of the finished product.

The preliminary experimental results show that the following control factors have the greatest effect.

1. Substrate speed: when the substrate contacts the roller, the UV resin has not yet cured. If the plate moves too fast, the roller slips and the microstructure is not accurately formed.
2. Exposure time: if the UV irradiation time is too short, the UV resin is not completely cured. If the irradiation time is long enough, the UV resin is completely cured. The substrate is warped and deformed if the irradiation time is too long.
3. Exposure position: the UV light source is located at the bottom of the roll-to-plate embossing machine. It emits UV light upwards through a transparent substrate to irradiate the UV resin. If the resin is exposed too early to ultraviolet light, the bottom layer of the UV resin cures (residual thickness will be produced) and the soft PDMS insert is compressed by the cured residual layer so the embossed microstructure is deformed and embossing is incomplete. The UV resin does not cure after embossing by the roller if it is exposed to UV

**Table 9** Variation analysis for DOT-3 microstructures

| Factor | SS | DOF | Contribution | Var | F | Confidence | Significant?[a] |
|---|---|---|---|---|---|---|---|
| A | 30.87 | 2 | 29.50% | 15.43 | 31.09 | 100.00% | Yes |
| B | 28.98 | 2 | 27.69% | 14.49 | 29.19 | 100.00% | Yes |
| C | 22.54 | 2 | 21.54% | 11.27 | 22.70 | 100.00% | Yes |
| D | 13.33 | 2 | 12.73% | 6.66 | 13.42 | 99.97% | Yes |
| Error | 8.94 | 18 | 8.54% | 0.50 | | S = 0.70 | |
| Total | 104.65 | 26 | 100.00% | | | | |

[a]At least 99% confidence level

**Table 10** Variation analysis for pyramid microstructures

| Factor | SS | DOF | Contribution | Var | F | Confidence | Significant?[a] |
|---|---|---|---|---|---|---|---|
| A | 61.95 | 2 | 13.21% | 30.98 | 273.96 | 100.00% | Yes |
| B | 81.39 | 2 | 17.35% | 40.69 | 359.90 | 100.00% | Yes |
| C | 154.68 | 2 | 32.98% | 77.34 | 684.04 | 100.00% | Yes |
| D | 168.93 | 2 | 36.02% | 84.47 | 747.05 | 100.00% | Yes |
| Error | 2.04 | 18 | 0.43% | 0.11 | | S = 0.34 | |
| Total | 468.99 | 26 | 100.00% | | | | |

[a]At least 99% confidence level

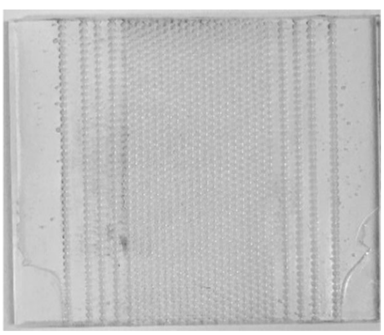

**Fig. 16** Light guide plate with DOT-3 microstructure

light too late. The UV resin remains uncured after leaving the roller so the microstructure is not completely formed. Exposure must start at an appropriate time to ensure that the process is effective.

4. Air pressure: adjusting the downward pressure of the cylinder arms on both sides adjusts the contact force between the roller and the substrate. This contact force affects the embossed height and the ease of demolding.

For the roll-to-plate UV-curing embossing processes, the Taguchi method was used to optimize the process parameters. The replicability of embossing for the finished

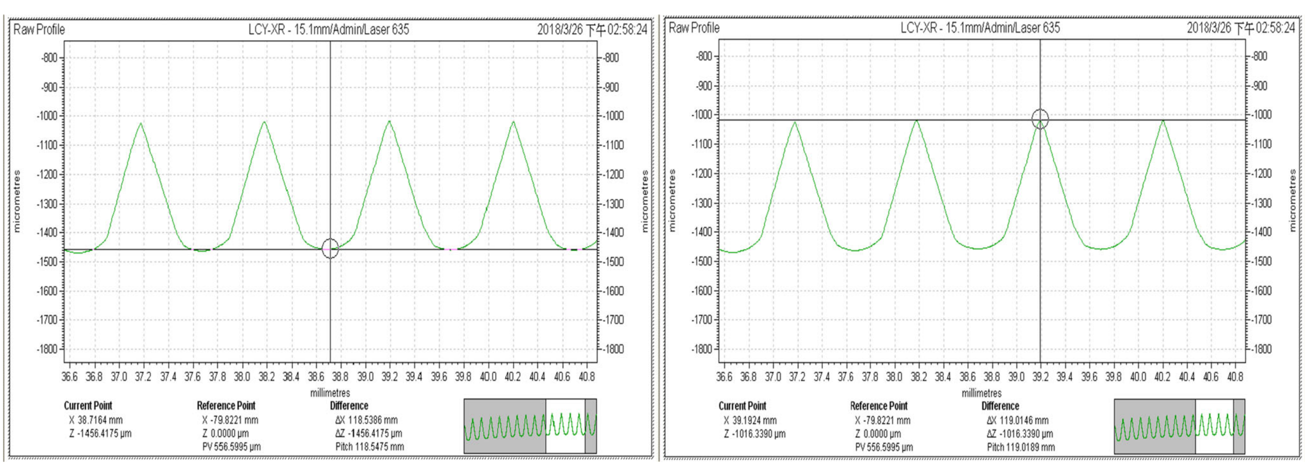


**Fig. 17** Measured profiles for DOT-3 microstructure using optimized parameters

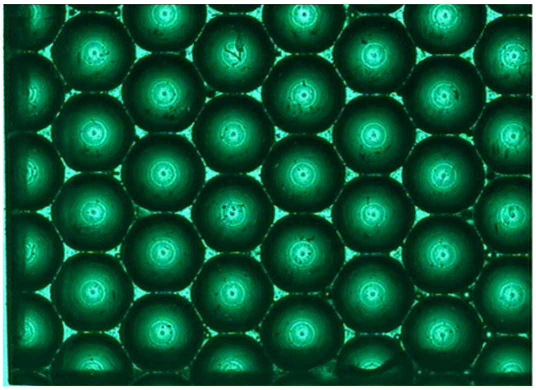

Fig. 18 DOT-3 microstructures (2.5D image measurement)

product was the quality characteristic. Four factors and three levels were used. The control factors for this study are substrate speed (A), exposure time (B), exposure position (C) and air pressure (D).

This experiment used DOT-3 and pyramid. The optimized exposure positions for these two structures are different. The factors and levels are shown in Tables 5, 6. The only difference is the level of exposure. An L9 orthogonal array was used for this Taguchi analysis. Each embossing experiment was conducted three times and the embossed height of the microstructure was measured at five points. An average of the results was used. In order to optimize the replicability of embossing for the product, the “the larger, the better” characteristic was used:

$$S/N = -10\log_{10}\frac{\sum_{i=1}^{n}\frac{1}{y_i^2}}{n}, \tag{1}$$

where $y_i$ is the embossing replicability, which is the ratio of the embossed height of the microstructure to the microstructure of the roller. Maximizing the *S/N* ratio gives an embossing replicability that is closest to the target value and minimizes the effect of noise.

The measured quality characteristics and the calculated *S/N* ratio are respectively shown in Tables 7 and 8 for DOT-3 and pyramid microstructures. The results of the variation analysis are shown in Tables 9 and 10. The table for variance analysis shows that these four factors have a significant influence on the replicability of as DOT microstructure and a pyramid microstructure.

For the DOT-3 microstructure, the contribution of factor A (substrate speed) is the greatest at 29.5%, followed by factor B (exposure time) at 27.69% and factor C (exposure position) at 21.54%. Factor D (air pressure) has the lowest contribution at 12.73%. For roll-to-plate embossing, the greater structural depth of DOT-3 means that the substrate speed is the most important factor. If the speed is slow, curing occurs too early because there is excessive

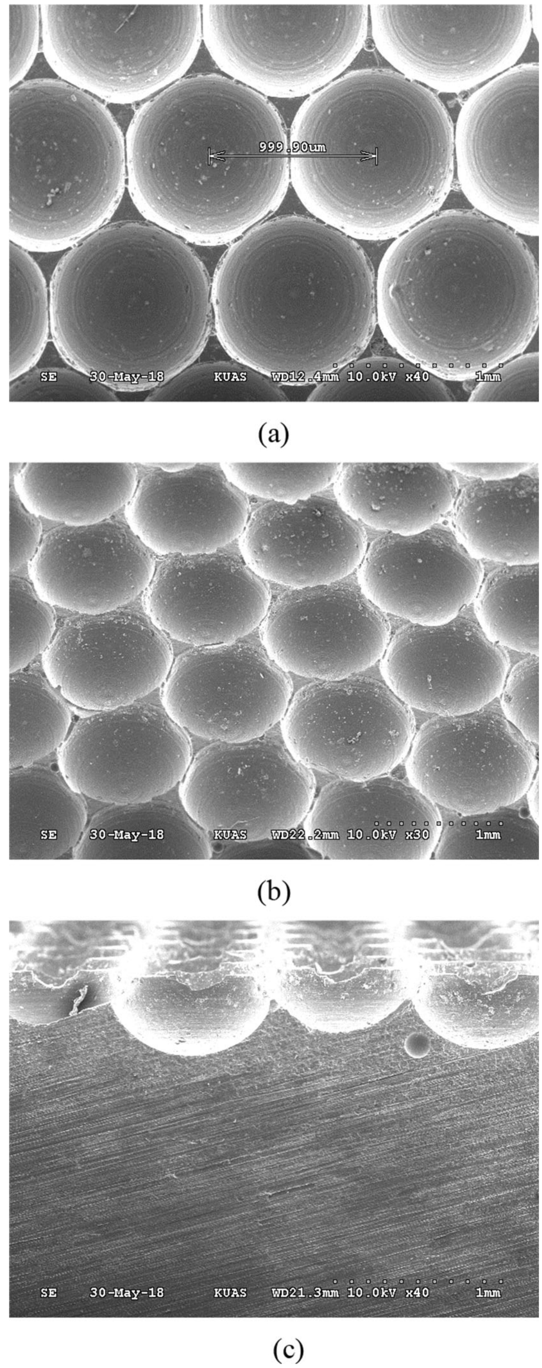


Fig. 19 SEM images of DOT-3 microstructures from different viewing angles

ultraviolet radiation energy, so the structure not completely embossed.

For the pyramid microstructure, the contribution of factor D (air pressure) is the greatest at 36.02, followed by factor C (exposure position) at 32.98% and factor B (exposure time) at 17.35%. Factor A (substrate speed) has the lowest contribution at 13.21%. The structure is concave so air pressure is the most important factor in ensuring that the

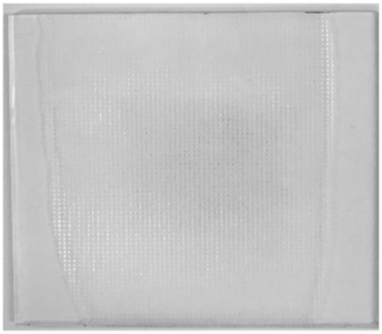

**Fig. 20** Light guide plate with pyramid microstructure

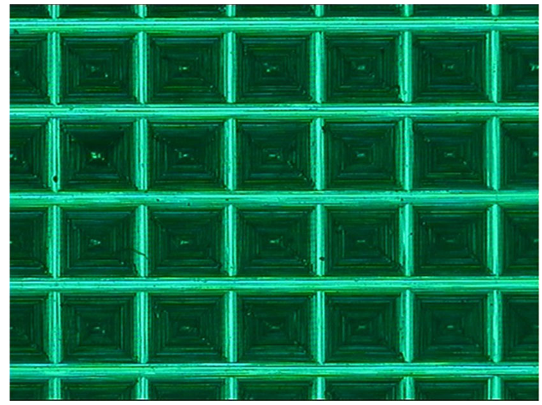

**Fig. 22** Pyramid microstructures (2.5D image measurement)

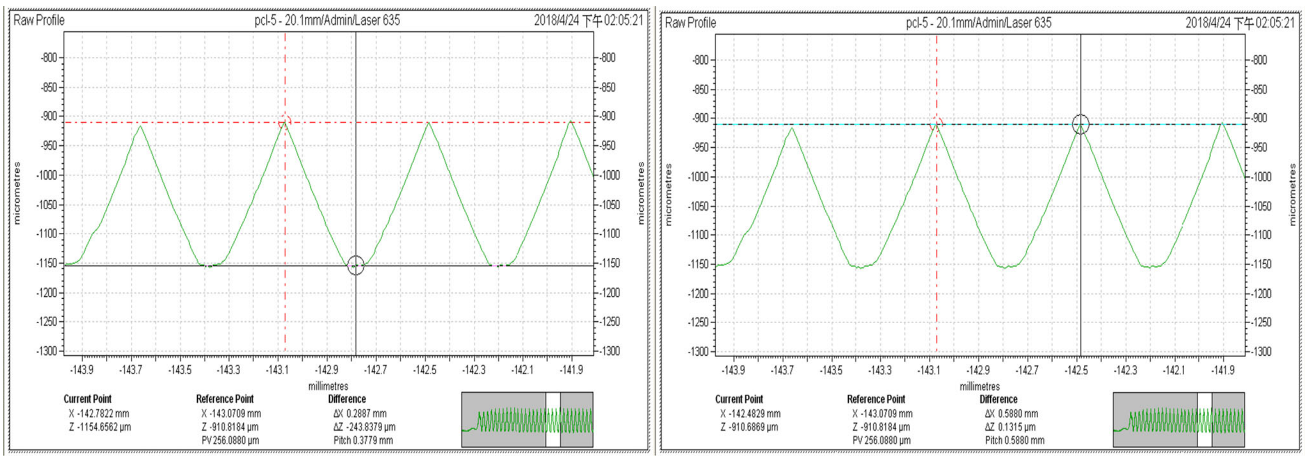


**Fig. 21** Measured profiles for pyramid microstructures using optimized parameters

UV resin fills the grooves during the roll-to-plate embossing process.

## 4 Results

The experimental data table and the factor response plot are used to determine the best combination of factors. The *S/N* ratio is used to predict the quality characteristics (replicability) at the optimal levels. Confirmation experiments were performed to measure the replicability at the optimal levels and the predicted value is compared with the experimental value.

The optimized parameters for the DOT-3 structure are A3 (4.5 mm/s), B2 (1 s), C3 (16 mm) and D1 (637 kPa). The light guide plate is shown in Fig. 16 and is obtained using roll-to-plate UV-curing embossing. The average height of the microstructure is 440 μm, as shown in Fig. 17. The replicability is 97.77% and the predicted value is 96.24%. The difference is 1.53%. Embossing using the optimized parameters for the DOT-3 structure gives the surface structure that is shown in Fig. 18. SEM photographs at different angles to the microstructures are shown in Fig. 19.

The optimized parameters for the pyramid structure are A2(3.6 mm/s), B1(0.75 s), C1(15 mm) and D2(686 kPa). The composite light guide plate is shown in Fig. 20 and is obtained using roll-to-plate UV-curing embossing. The average height of the microstructure is 243 μm, as shown in Fig. 21. The replicability is 97.26%, and the predicted value is 96.96%. The difference is 0.24%. Embossing using the optimized parameters for the pyramid structure gives the surface structure that is shown in Fig. 22. SEM photographs at different angles to the microstructures are shown in Fig. 23.

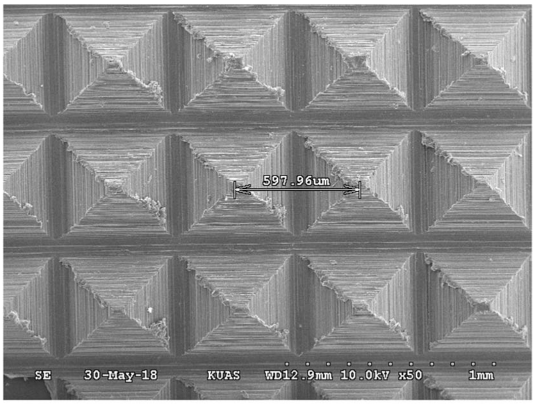


(a)

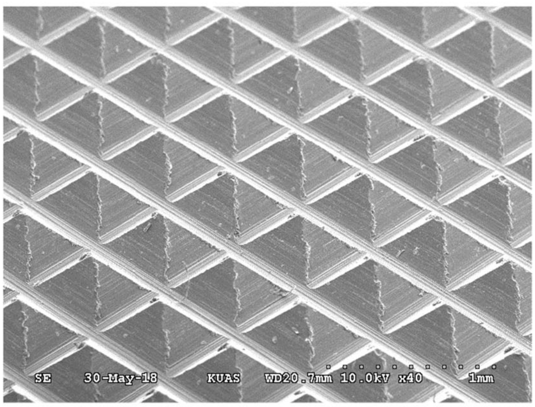


(b)

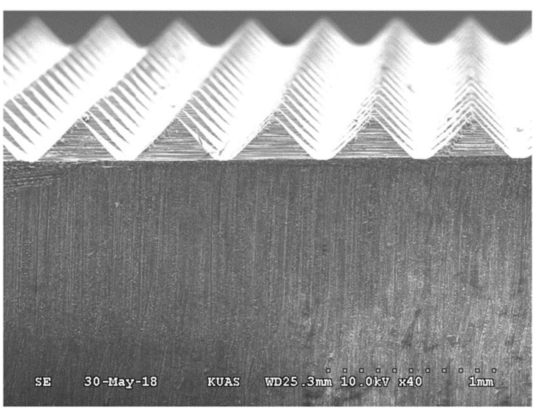


(c)

**Fig. 23** SEM images of pyramid microstructures from different viewing angles

The most important optical property for this experiment is the luminance of the light guide plate. Four types of microstructures were produced using roll-to-plate UV-curing embossing—no-structure, DOT-3, pyramid and composite type—as shown in Fig. 24. The light guide plates were installed in a homemade backlight module, as shown in Fig. 25. The luminance was measured using a luminance meter and the measured values are shown in Figs. 26, 27, 28 and 29. The measured luminance at nine points is shown in Table 11. The luminance of the center point is used as the standard to determine the relative luminance values.

## 5 Conclusions

This study uses optical simulation technology to design a composite light guide plate. Roll-to-plate UV-curing embossing technology is used to form DOT microstructures and pyramid microstructures. This method has a short molding cycle and can continuously produce a large number of composite light guide plates with double-sided microstructures.

The luminance measurements at nine points show that the composite type has a luminance that is 9.4 times higher than that for an unstructured type. The luminance distribution for the composite type is significantly more uniform than that for the unstructured type and the light is uniformly distributed as expected.

The Taguchi experiment shows that factor A (substrate speed), factor B (exposure time), factor C (exposure position) and factor D (air pressure) all have a significant effect on microstructure embossing. Rolling experiments using the optimized parameters show that the DOT microstructure and the pyramid microstructure can be replicated 97%.

To produce a light guide plate with a composite structure, the first side of the DOT-3 microstructure is rolled and then the second side with the pyramid microstructure. The rolling on both sides uses the optimized parameters for the microstructure. When rolling the second surface, the microstructure of the first surface has a slight effect on the penetration of UV light. The replicability of the second side is 96.3% so the difference is not significant.

The measurement results for luminance for the four types of light guide plates—unstructured, DOT-3, pyramid

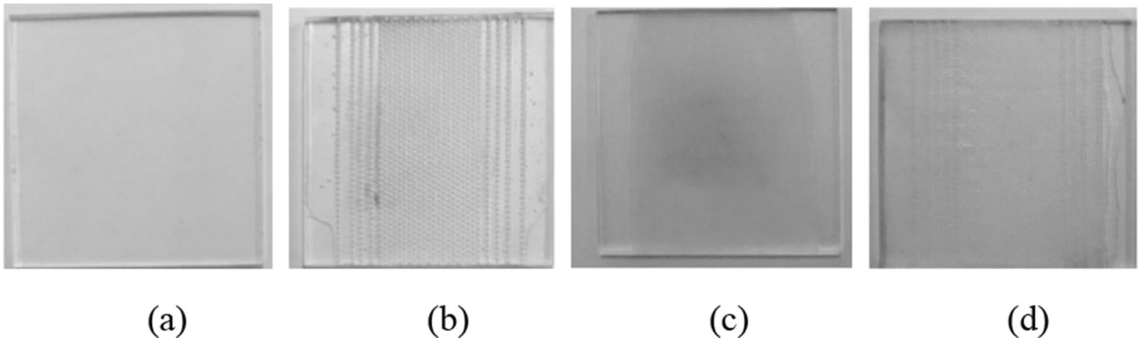


**Fig. 24** LGPs with (**a**) no-structure, (**b**) DOT-3, (**c**) pyramid and (**d**) composite type

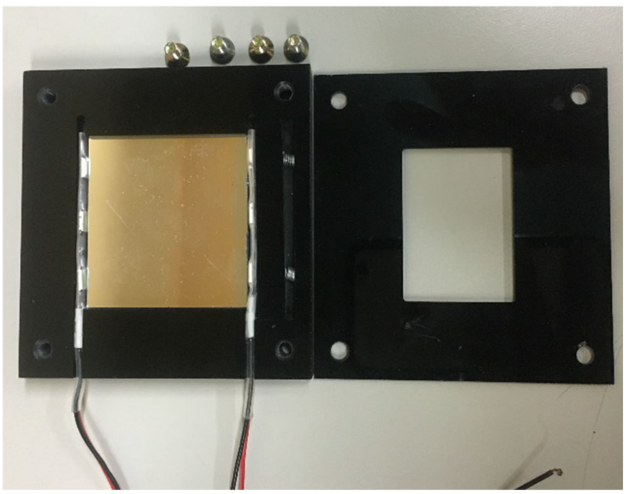

**Fig. 25** LGP installed in a homemade backlight module

and composite show that the maximum luminance and the minimum luminance of the composite light guide plate differ by 23% so greater uniformity of luminance is obtained for a thinner composite light guide plate.

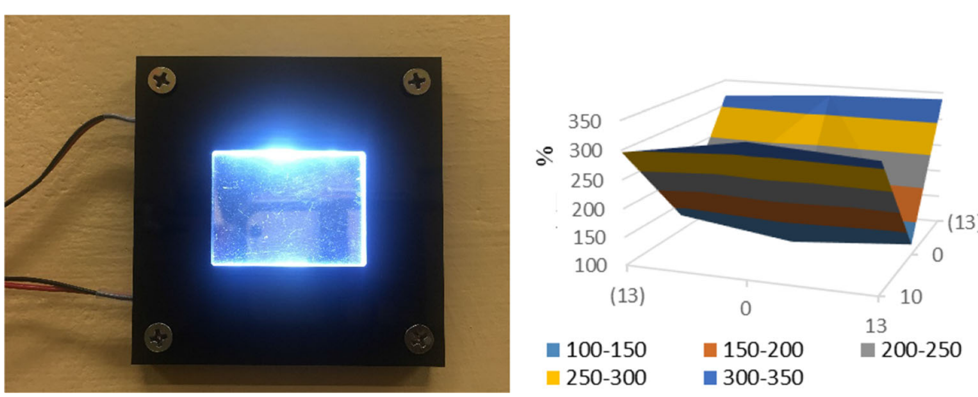


**Fig. 26** Luminance of LGP with no microstructures

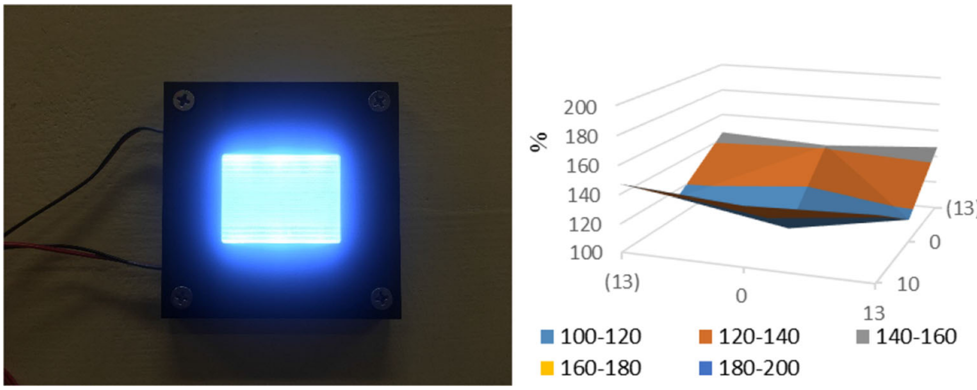


**Fig. 27** Luminance of LGP with DOT-3 microstructure

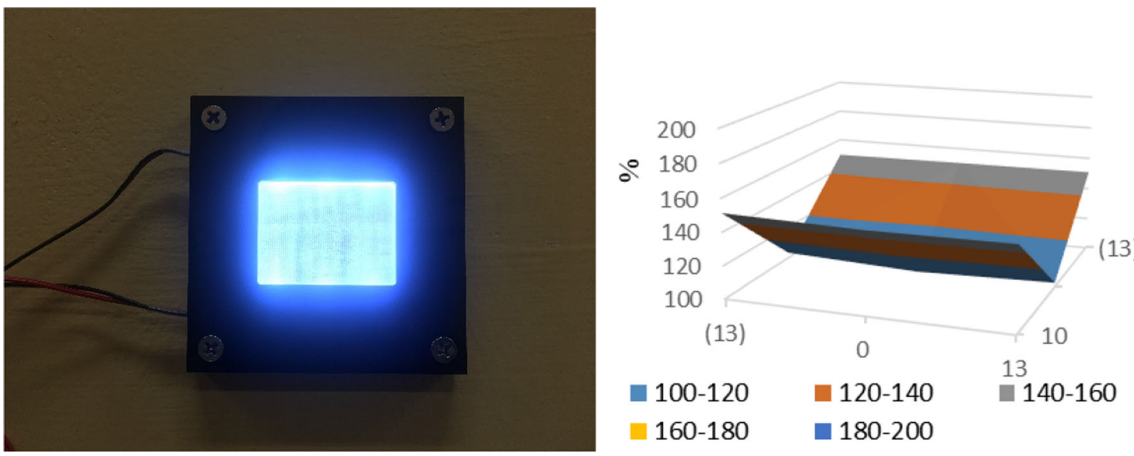


**Fig. 28** Luminance of LGP with pyramid microstructure

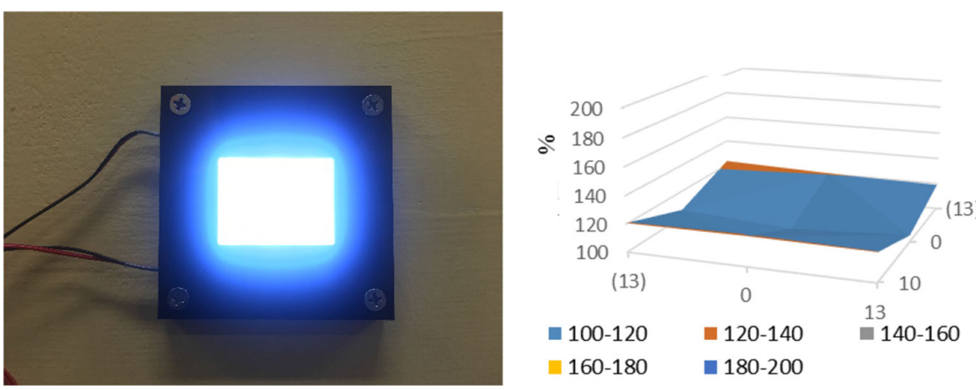


**Fig. 29** Luminance of the composite LGP

**Table 11** The luminance measurement results for nine points on the composite LGP

| Luminance at 9 points | | | | Relative luminance (%) | | |
|---|---|---|---|---|---|---|
| 1945 | 1953 | 1941 | | 121 | 121 | 120 |
| 1699 | 1611 | 1687 | Average | 105 | 100 | 105 |
| 1983 | 1941 | 1916 | 1853 | 123 | 120 | 119 |

**Acknowledgements** This work was supported by the Ministry of Science and Technology under MOST grant—MOST 109-2221-E-992-003.

## References

Chan-Park MB, Neo WK (2003) Ultraviolet embossing for patterning high aspect ratio polymeric microstructures. Microsyst Technol 9(6–7):501–506

Wu C-H, Lu C-H (2008) Fabrication of an LCD light guide plate using closed-die hot embossing. J Micromech Microeng 18(3):035006

Feng D, Jin G, Yan Y, Fan S (2004) High quality light guide plates that can control the illumination angle based on microprism structures. Appl Phys Lett 85(24):6016–6018

Gates BD, Xu QB, Stewart M, Ryan D, Willson CG, Whitesides GM (2005) New approaches to nanofabrication: molding, printing, and other techniques. Chem Rev 105:1171–1196

Heckele M, Bacher W, Muller KD (1998) Hot embossing—the molding technique for plastic microstructures. Microsyst Technol 4(3):122–124

Nezuka O, Yao D, Kim BH (2008) Replication of microstructures by roll-to-roll UV-curing embossing. Polym Plastics Technol Eng 47:865–873

Yang J-C, Huang C-C (2013) Fabrication of dual brightness enhancement structures on light guide plates using UV roll-to-plate imprint lithography. Optik 124(18):3324–3328

Yao D, Kim B (2002) Injection molding high aspect ratio microfeatures. J Injection Molding Technol 6:11–17

Yeo LP, Joshi SC, Lam YC, Chan-Park MB, Hardt DE (2009) Numerical analyses of peel demolding for UV embossing of highaspect ratio micro-patterning. Microsyst Technol 15(4):581–593

Zhong ZW, Shan XC (2014) A study of meniscus formation and its effect on roll-to-roll UV embossing. Intern J Eng Sci 85:10–19